OPEN ACCESS
CellPress

Cell Reports
Resource

# Isolation of Chromatin from Dysfunctional Telomeres Reveals an Important Role for Ring1b in NHEJ-Mediated Chromosome Fusions

Cristina Bartocci,[1] Jolene K. Diedrich,[2] Iliana Ouzounov,[1] Julia Li,[1] Andrea Piunti,[3] Diego Pasini,[3] John R. Yates III,[2] and Eros Lazzerini Denchi[1,*]
[1]Department of Molecular and Experimental Medicine, The Scripps Research Institute, La Jolla, CA 92037, USA
[2]Department of Chemical Physiology, The Scripps Research Institute, La Jolla, CA 92037, USA
[3]Department of Experimental Oncology, European Institute of Oncology, 20146 Milan, Italy
*Correspondence: edenchi@scripps.edu
http://dx.doi.org/10.1016/j.celrep.2014.04.002


## SUMMARY

**When telomeres become critically short, DNA damage response factors are recruited at chromosome ends, initiating a cellular response to DNA damage. We performed proteomic isolation of chromatin fragments (PICh) in order to define changes in chromatin composition that occur upon onset of acute telomere dysfunction triggered by depletion of the telomere-associated factor TRF2. This unbiased purification of telomere-associated proteins in functional or dysfunctional conditions revealed the dynamic changes in chromatin composition that take place at telomeres upon DNA damage induction. On the basis of our results, we describe a critical role for the polycomb group protein Ring1b in nonhomologous end-joining (NHEJ)-mediated end-to-end chromosome fusions. We show that cells with reduced levels of Ring1b have a reduced ability to repair uncapped telomeric chromatin. Our data represent an unbiased isolation of chromatin undergoing DNA damage and are a valuable resource to map the changes in chromatin composition in response to DNA damage activation.**

## INTRODUCTION

Most human cancer cells have short telomeres when compared to normal surrounding tissues (Hastie et al., 1990; Meeker et al., 2004). This is due to the relatively late reactivation of telomerase during tumorigenesis, resulting in the proliferation of cells for an extended period of time in the absence of a telomere elongation mechanism (Maser and DePinho, 2002; Shay and Wright, 2001). Loss of end protection is frequently detected in human cancers such as colorectal carcinomas (Rudolph et al., 2001), oral squamous cell carcinomas (Gordon et al., 2003), and chronic lymphocytic leukemia (Augereau et al., 2011; Chin et al., 2004; Lin et al., 2010; Suram et al., 2012). Mounting evidence suggests that telomere dysfunction plays a crucial role in promoting tumor development (Ramsay et al., 2013). For example, the induction of telomere dysfunction in mice results in epithelial cancers with a complex karyotype, indicative of rampant genomic instability (Artandi et al., 2000; Chin et al., 1999). The most striking illustration of the role of end protection in human health comes from patients affected by the rare inherited disorder dyskeratosis congenita (DC). This disease is caused by mutations affecting either telomere elongation factors (dyskerin and hTERT) or telomere-associated proteins (Dokal, 2000; Kirwan and Dokal, 2009; Mitchell et al., 1999; Sarper et al., 2010; Shay and Wright, 1999; Touzot et al., 2010; Vulliamy et al., 2004; Walne et al., 2008). Among other symptoms, DC patients have critically short telomeres, show signs of telomere dysfunction, and display an increased incidence of cancer.

When telomeres become critically short, they fail to recruit sufficient levels of protective shelterin complex, resulting in failure to protect chromosome ends and leading to the activation of a DNA damage response (DDR) pathway (d'Adda di Fagagna et al., 2003; Takai et al., 2003). Indeed, to date, the following DNA damage proteins have been shown to play a role in the response to dysfunctional telomeres: MRE11, ATM, γH2AX, MDC1, RNF8, RNF168, 53BP1, RIF1, and PTIP1 (Attwooll et al., 2009; Chapman et al., 2013; Denchi and de Lange, 2007; Di Virgilio et al., 2013; Dimitrova et al., 2008; Dimitrova and de Lange, 2006, 2009; Peuscher and Jacobs, 2011; Zimmermann et al., 2013). However, a global approach to systematically determine which factors relocalize to or from dysfunctional telomeres is currently lacking.

Here, we applied a proteomic approach to comprehensively characterize the proteins whose localization changes upon telomere dysfunction. Using this approach, we identified a series of previously characterized DDR factors as telomere-dysfunction-recruited factors in addition to a set of factors that are recruited to dysfunctional telomeres. In addition, our data revealed a critical role for the polycomb protein Ring1b for the efficient nonhomologous end-joining (NHEJ)-mediated fusion of dysfunctional telomeres.

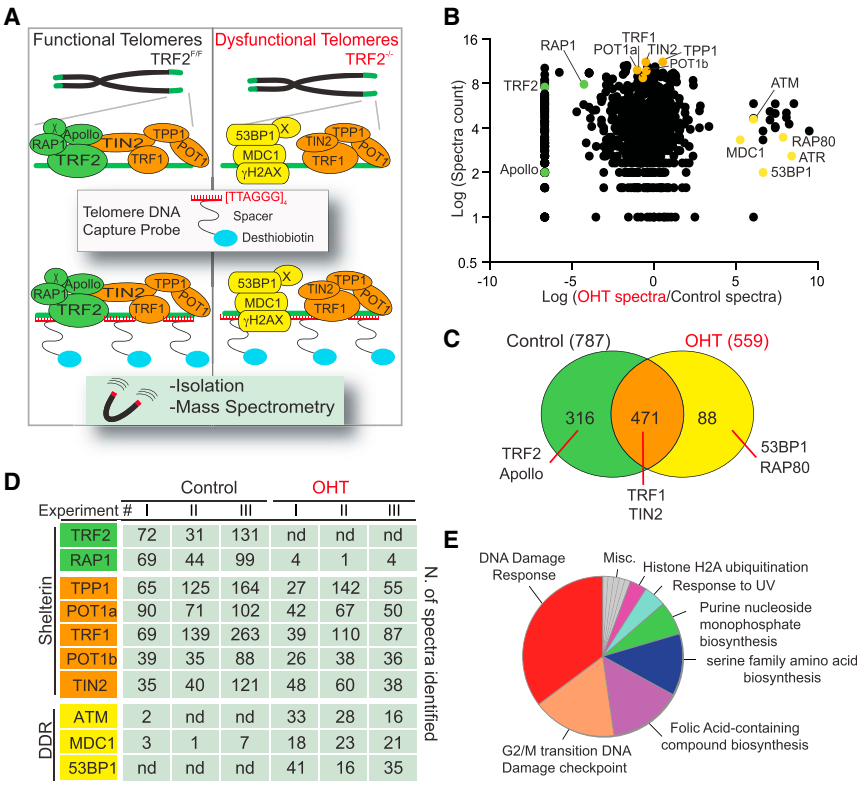


**Figure 1. Proteomics of Isolated Chromatin Segments of Functional and Dysfunctional Mouse Telomeres**

(A) Schematic representation of the PICh analysis employed to define the chromatin changes that occur at telomeres upon TRF2 depletion.

(B) Identified proteins were plotted based on the log2 intensity (y axis) calculated based on the total spectra counts identified and ratio between TRF2-proficient and TRF2-deficient settings (x axis) calculated as log2 (OHT spectra/control spectra). Only proteins identified in at least two experiments are plotted. Green and orange dots represent proteins recruited at telomeres in a TRF2-dependent or TRF2-independent manner, respectively. Yellow dots represent known DNA damage factors recruited to dysfunctional telomeres.

(C) Venn diagrams depicting the total number of proteins identified in at least two out of three PICh experiments from the control and OHT samples and the degree of overlap between the data sets from the two samples.

(D) Table listing shelterin components and some of the DNA damage response (DDR) factors identified with the corresponding spectra counts isolated in each individual experiment. nd, not detected.

(E) Pie chart illustrating the distribution of proteins identified in the TRF2-depleted samples (OHT), classified according to Gene Ontology (GO). Note the enrichment for DNA damage response proteins.

## RESULTS

### Changes in Chromatin Composition following Telomere Dysfunction

We hypothesized that upon acute telomere dysfunction, relocalization of DDR factors at telomeric repeats $[TTAGGG]_n$ would lead to a drastic change in chromatin composition at chromosome ends and that this could be isolated and identified using an unbiased proteomic approach. To verify this hypothesis, we adapted a technique termed PICh (proteomics of isolated chromatin segments) that allows the isolation of chromatin regions using a biotinylated oligonucleotide complementary to a DNA sequence of interest (Déjardin and Kingston, 2009). PICh was originally designed to isolate telomeric chromatin derived from human cells and employed locked nucleic acid (LNA)-modified oligos. We optimized several steps in the PICh protocol in order to efficiently isolate telomeric chromatin from murine cells including the use of peptide nucleic acid (PNA)-modified oligonucleotides as capture probes. In our experiments, the use of PNA probes resulted in more efficient isolation of telomeric chromatin when compared to LNA-modified oligonucleotides (data not shown). To achieve synchronous and homogenous telomere dysfunction, we used TRF2 conditional knockout mouse embryonic fibroblasts (MEFs) (Celli and de Lange, 2005) harboring an inducible CRE recombinase (Rosa26-CRE-ER) (previously described in Okamoto et al., 2013). 4-Hydroxytamoxifen (OHT) treatment of these cells allows for efficient and synchronous deletion of TRF2, resulting in DNA damage activation at every chromosome end (Okamoto et al., 2013). Telomeric chromatin was isolated using a PNA capture probe complementary to the telomeric repeat sequence $[TTAGGG]_3$ conjugated with a desthiobiotin moiety (see Figure 1A for schematics). Telomeric chromatin was isolated in three independent experiments from TRF2-depleted (OHT) and control cells. The resulting chromatin-associated proteins were identified using liquid chromatography tandem mass spectrometry, and only proteins identified in at least two independent experiments were further analyzed. In total, we identified 787 unique proteins in samples derived from TRF2-proficient cells and 559 in samples derived from TRF2-deficient cells (Figure 1; Table S1). Importantly, despite the different cellular systems used, there is 60% of overlap between the proteins that we identified in TRF2-proficient MEFs and the ones isolated in HeLa cells (Déjardin and Kingston, 2009). In support of our initial hypothesis, we found significant differences in the composition of telomeric chromatin in the presence or absence of TRF2, with 316 proteins found only at TRF2-proficient telomeres, 88 proteins found only at TRF2-deficient telomeres, and 471 proteins found in both conditions (Figure 1C). Among the proteins that were only found at TRF2-proficient telomeres, we found TRF2 and its binding partners RAP1 and Apollo (Lenain et al., 2006; van Overbeek and de Lange, 2006; Li et al., 2000) (Figures 1B–1D; Table S2). In contrast, from TRF2-deficient telomeres, we isolated several DNA damage factors that have been previously shown to localize to dysfunctional telomeres such as ATM, the MRE11 complex, MDC1, and 53BP1 (Celli and de Lange, 2005; Dimitrova and de Lange, 2006) (Figures 1B–1D; Table S3). Finally, proteins that are known to bind to telomeres in a TRF2-independent manner

A

| Gene | OHT spectra | NT spectra | ΔSpectra | Rank |
|---|---|---|---|---|
| Atm | 26 | 1 | 1.0 | 1 |
| Topbp1 | 11 | 5 | 0.6 | 2 |
| Wrn | 1 | nd | 1.0 | 3 |
| Mdc1 | 21 | 4 | 0.8 | 4 |
| 53BP1 | 31 | 3 | 0.9 | 5 |
| Atr | 3 | nd | 1.0 | 8 |
| Rif1 | 8 | 4 | 0.5 | 14 |
| Mre11a | 16 | 3 | 0.8 | 18 |
| Nbn | 2 | 1 | 0.4 | 27 |
| Rad50 | 17 | 2 | 0.9 | 28 |
| Rad18 | 2 | nd | 1.0 | 10 |
| Fancd2 | 2 | nd | 1.0 | 15 |
| Rap80 | 2 | nd | 1.0 | 19 |
| Senp7 | 1 | nd | 0.7 | 21 |
| Timeless | 1 | nd | 0.8 | 22 |
| Pml | 4 | 1 | 0.7 | 24 |
| Rnf213 | 2 | nd | 1.0 | 37 |
| Stag2 | 5 | 2 | 0.7 | 41 |
| Matr3 | 35 | 19 | 0.4 | 52 |
| Nvl | 1.3 | nd | 1.0 | 60 |
| Ring1b | 2.3 | 1 | 0.4 | 65 |
| D1Pas1 | 2.6 | 1.3 | 0.5 | 66 |
| Dusp3 | 1.6 | 0.7 | 0.6 | 76 |
| Fam50a | 1 | 0.3 | 0.7 | 85 |
| Ppp2r5d | 1 | 0.3 | 0.7 | 90 |

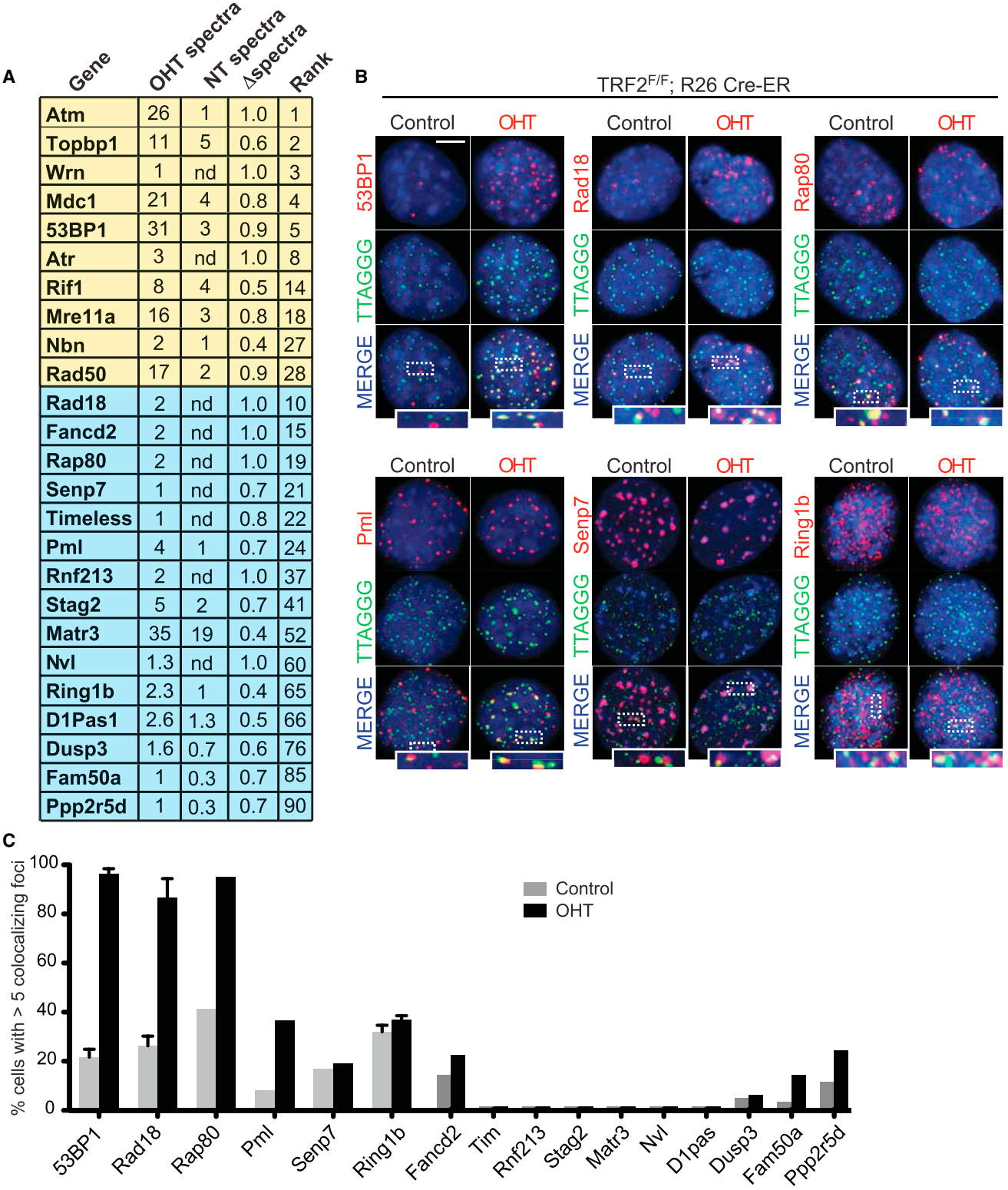


**Figure 2. Validation of Factors that Localize at Dysfunctional Telomeres**

(A) List of proteins identified by PICh as enriched at dysfunctional telomeres. Average number of spectra identified at TRF2-deficient (OHT) or TRF2-proficient (NT) telomeres is indicated. Proteins were ranked based on their relative enrichment at TRF2-depleted telomeres and normalized to absolute expression of the protein

*(legend continued on next page)*

were not significantly enriched in either sample, such as the shelterin components (TRF1, TIN2, TPP1, POT1a, and POT1b) and other known telomere-associated proteins, such as members of the STN1 and THO complexes and the chromatin-remodeling factors ATRX and DAXX (Figures 1B–1D; Table S1) (Buscemi et al., 2004; de Lange, 2005; Lewis et al., 2010; Pfeiffer et al., 2013; Wong et al., 2010). Annotation of the proteins found only in the TRF2-depleted setting revealed a significant enrichment for DDR genes (Figure 1E). Collectively, our data show that using a PICh-based approach, we were able to detect the changes that occur in chromatin upon removal of the telomeric factor TRF2 and the consequent induction of a DNA damage response at uncapped chromosome ends.

## Isolation of Proteins that Are Displaced from Dysfunctional Telomeres

To define the critical changes that occur in telomeric chromatin upon removal of TRF2, we first focused on the proteins that were lost upon OHT treatment. To this end, proteins with significant telomeric enrichment in TRF2-proficient cells relative to OHT-treated controls were ranked based on their absolute expression in mouse cells using the online database PaxDB (Wang et al., 2012). In addition, the resulting lists were run against the Contaminant Repository for Affinity Purification (http://www.crapome.org) (Mellacheruvu et al., 2013), and common contaminants were excluded from further analysis. Significantly, the list of proteins that are lost upon TRF2 depletion contained at top-ranking positions RAP1 and Apollo, two proteins that have been shown to be recruited at telomeres in a TRF2-dependent manner (Celli and de Lange, 2005; Lenain et al., 2006; Li et al., 2000; van Overbeek and de Lange, 2006), as well as TRF2 (Table S2). To validate additional factors that are lost from telomeres upon TRF2 depletion, we chose two proteins among the top 5% of the factors enriched at TRF2-proficient telomeres: LRWD1 and CDCA8. Localization of these proteins at telomeres was tested in the presence or absence of TRF2 using tagged alleles expressed from retroviral vectors in $TRF2^{F/F}$ Rosa26 CRE-ER MEFs. As a positive control, we used a myc-tagged RAP1 allele. Our results indicate that CDCA8 and LRWD1 showed frequent colocalization with telomeric DNA (Figures S1A and S1B). In agreement with our PICh results, we found that upon TRF2 depletion, the localization of CDCA8 with telomeres was reduced by approximately 50% (Figure S1B). On the contrary, LRWD1 localization to telomeres was not significantly affected by the loss of TRF2, suggesting that its recruitment to telomeres is independent of TRF2 (Figure S1B). Therefore, these data suggest that our analysis can detect both known and unidentified telomere-associated factors that are affected by TRF2 depletion. Interestingly, LRWD1 was also recently identified at telomeres in a quantitative proteomic approach performed by the Lingner laboratory (Grolimund et al., 2013). To address whether CDCA8 and/or LRWD1 play a critical role in telomere protection, we performed small hairpin RNA (shRNA) depletion of these proteins. Efficient downregulation of either CDCA8 or LRWD1 did not result in accumulation of the DNA damage factors γH2AX and 53BP1 at telomeres (Figures S1C–S1E). In contrast, shRNA-mediated downregulation of TRF2 resulted in frequent localization of γH2AX and 53BP1 foci at chromosome ends (Figures S1C–S1E). CDCA8 is part of the chromosome passenger complex (CPC), which is involved in proper mitotic segregation and cytokinesis (reviewed in Carmena et al., 2012). LRWD1 mediates association of the origin recognition complex (ORC) to chromatin and was shown to be required for the maintenance of pericentric heterochromatin silencing (Chan and Zhang, 2012; Shen et al., 2010). Although depletion of these proteins did not result in activation of a DNA damage response at TRF2-depleted telomeres, we could not exclude that CDCA8 and/or LRWD1 have a role at telomeres that was not detected by our analyses, and further functional characterization is currently undergoing and will be reported in a future study.

## Isolation of Proteins that Are Recruited to Dysfunctional Telomeres

Next, we focused on factors that are recruited to telomeres following TRF2 loss. Proteins were ranked based on their relative enrichment at dysfunctional telomeres and normalized to their absolute expression in mouse cells (Wang et al., 2012). This analysis revealed 114 proteins that are enriched at TRF2-depleted telomeres. Among these proteins, we found 24 known DDR proteins, of which ten were previously reported to be associated with dysfunctional telomeres (Figure 2A; Table S3). To validate whether our approach identified factors that relocalize to dysfunctional telomeres, we selected 15 proteins ranked at different positions within this list and tested their localization in the presence or absence of TRF2 (Figure 2). The selected factors represented both proteins that were previously shown to interact with DNA damage sites as well as proteins with no reported link to the DDR pathway. $TRF2^{F/F}$ Rosa26 CRE-ER MEFs expressing a tagged version of the selected proteins were treated with tamoxifen (OHT) or left untreated (control), and the localization of the ectopically expressed proteins to telomeric DNA was assessed by indirect immunofluorescence (IF). As a positive control, we used a 53BP1 allele that has been previously shown to localize to dysfunctional telomeres (Dimitrova et al., 2008). As expected, ectopically expressed 53BP1 colocalized with telomeres in the vast majority of TRF2-deficient cells (Figures 2B and 2C). Similarly, eight of the selected proteins (Rad18, Rap80, Senp7, Ring1b, Pml, Fam50a, Fancd2, and Ppp2r5d) localized at telomeres upon TRF2 depletion, while the remaining seven showed

in mouse cells (PaxDB database). Proteins highlighted in yellow represent DNA damage response factors known to localize at dysfunctional telomeres. Proteins highlighted in blue represent proteins selected for validation.

(B) Localization of ectopically expressed tagged proteins (myc/GFP) (stained in red) to telomere repeats (TTAGGG, stained in green). $TRF2^{F/F}$ Rosa26 CRE-ER MEFs infected with the indicated constructs were treated with OHT and harvested 3 days later. Scale bar represents 5 μm.

(C) Quantification of data shown in (B). Cells with five or more foci colocalizing with telomeres were counted as positive. Error bars represent SD of average of three independent experiments.

See also Figure S2.

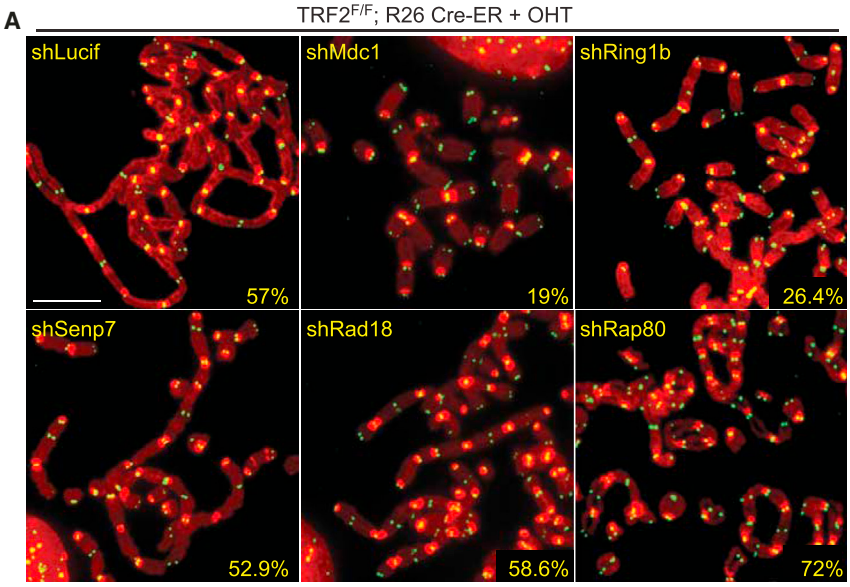


B

| shRNA | Telomeres | Fused Telomeres | p value |
|---|---|---|---|
| shLucif | 6268 | 3570 | control |
| shMdc1 | 2004 | 382 | < 0.0001 |
| shRing1b | 4500 | 1190 | < 0.0001 |
| shSenp7 | 1480 | 784 | > 0.05 |
| shRad18 | 4264 | 2490 | > 0.05 |
| shLucif#2 | 1996 | 1434 | control |
| shRap80 | 1088 | 812 | > 0.05* |

*relative to shLucif#2

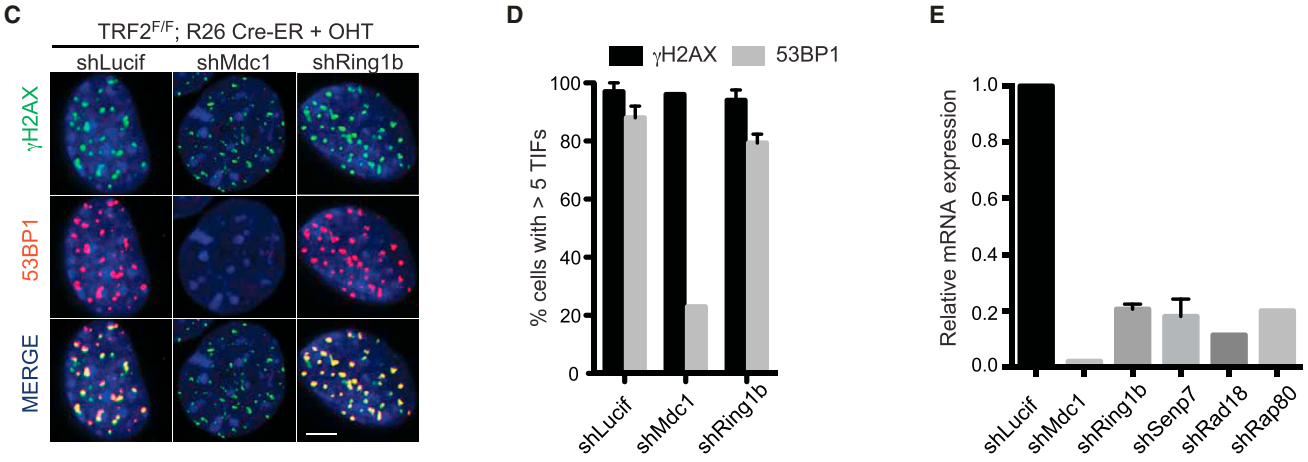


**Figure 3. Ring1b Plays a Critical Role in the Response to Dysfunctional Telomeres**

(A) Metaphase spreads were harvested from TRF2$^{F/F}$ Rosa26 CRE-ER MEFs infected with a control lentiviral construct (shLuciferase) or with the indicated shRNA constructs and treated with OHT for 96 hr. Chromosomes were stained with a PNA probe complementary to telomeric repeats (green) and DAPI (red). Percentages of fused chromosome ends are indicated. Scale bar represents 5 μm.

(B) Quantification of data shown in (A).

(C) TRF2$^{F/F}$ Rosa26 CRE-ER MEFs infected with the indicated shRNA constructs were treated with OHT for 72 hr and fixed and stained for γH2AX (green), 53BP1 (red), and DAPI (blue). Scale bar represents 5 μm.

(D) Quantification of the data shown in (C) (cells with five or more γH2AX/53BP1 foci were counted as positive). Error bars represent SD of average of three independent experiments.

(E) Quantification of relative mRNA levels of the indicated genes in cells infected with the indicated shRNA constructs, normalized to shLuciferase as control. Error bars represent SD of the average of three independent experiments.

See also Figure S3.

either no detectable colocalization or a diffuse nuclear staining (Figures 2B and 2C). Nucleoplasmic extraction experiments revealed tight association of Rad18, Rap80, Pml, Senp7, Ring1b, and Fancd2 with dysfunctional telomeres (Figure S2).

## A Role for Ring1b in the Onset of End-to-End Chromosome Fusions

TRF2-depleted cells undergo dramatic end-to-end chromosome fusions (Celli and de Lange, 2005). To test whether any of the factors identified at TRF2-depleted telomeres plays a role in this process, we infected cells with specific shRNAs and tested the frequency of end-to-end chromosome fusions on metaphase spreads (Figure 3A). As a positive control, we used an shRNA directed against MDC1 that results in reduced levels of NHEJ-mediated telomere fusions (Dimitrova and de Lange, 2006). Strikingly, this analysis revealed that cells with reduced Ring1b expression showed approximately a 50% reduction in the rate of NHEJ-mediated telomere fusions (Figures 3A, 3B, and 3E).

In contrast, efficient knockdown of Rad18, Rap80, or Senp7 did not show a significant effect on the rate of telomere fusions. The effect of Ring1b on telomere fusion was further confirmed using telomere restriction fragment (TRF) analysis on Southern blots (Figure S3A). Importantly, we exclude that the observed defect in NHEJ efficiency reflects an alteration in cell-cycle progression caused by reduced Ring1b levels based on fluorescence-activated cell sorting (FACS) analysis (Figure S3B). To test whether the NHEJ defects observed upon Ring1b depletion could be due to altered DNA damage signaling at TRF2-deficient telomeres, we tested the induction of phosphorylated H2AX (γH2AX) and recruitment of 53BP1 in the TRF2$^{F/F}$ Rosa26 CRE-ER cells treated with tamoxifen and infected with the shRNA construct against Ring1b. As a control, we used a previously validated shRNA against MDC1 that affects the recruitment of 53BP1 at TRF2-depleted telomeres (Dimitrova and de Lange, 2006). Knockdown of Ring1b had no significant effect on the dynamics of γH2AX or 53BP1 to TRF2-depleted telomeres, while depletion of MDC1 resulted in impaired recruitment of 53BP1 as previously described (Figures 3C–3E). In addition, Ring1b depletion did not impair recruitment of the 53BP1 downstream effector RIF1 (Chapman et al., 2013; Escribano-Díaz et al., 2013; Zimmermann et al., 2013) to dysfunctional telomeres, excluding that the NHEJ defects observed in Ring1b-depleted cells are due to impaired RIF1 recruitment (Figures S3C and S3D). These experiments suggest that Ring1b might play a role at dysfunctional telomeres independent of the dynamics of γH2AX and 53BP1 at these sites.

To exclude the possibility that the observed phenotype is caused by an off-target effect, we generated an shRNA-resistant allele of Ring1b (Ring1b-WT*). Expression of Ring1b-WT* in TRF2-deficient cells infected with shRing1b rescued the NHEJ defects, thus excluding potential off-target effects (Figures 4A and S4A). Ring1b is a RING finger E3 ubiquitin ligase of the polycomb repressive complex 1 (PRC1) that acts in concert with Bmi1 to ubiquitinate histone H2A on K119 (H2AK119ub), via its RING finger domain, and to promote gene silencing and chromatin compaction (Cao et al., 2005; Stock et al., 2007; Vidal, 2009; Wang et al., 2004). In agreement with our observation that Ring1b localizes to chromosome ends, we observed an enrichment of the H2AK119ub mark at telomeres compared to other genomic loci by chromatin immunoprecipitation (ChIP) (Figures S4B–S4D). To test whether the enzymatic activity of Ring1b is required to promote NHEJ at TRF2-depleted cells, we complemented Ring1b-depleted cells with an shRNA-resistant, catalytically inactive mutant allele of Ring1b carrying a mutation in the RING domain (Ring1b-I53A*) (Buchwald et al., 2006). Expression of Ring1b-I53A* in TRF2-deficient cells rescues the NHEJ defect observed in the absence of Ring1b to levels that are comparable to ones observed in cells expressing the wild-type Ring1b-WT* allele (Figures 4A and S4A). These data indicate that the catalytic activity of Ring1b is dispensable for its role in promoting NHEJ at dysfunctional telomeres.

Next, we tested whether inhibition of Ring1b binding partner Bmi1 by shRNA would affect NHEJ-mediated telomere fusions. Indeed, expression of two independent shRNA constructs directed against Bmi1 resulted in a significant reduction in the rate of telomere fusions in TRF2 null cells (Figures 4B and 4C). Bmi1 inhibition did not affect phosphorylation of H2AX or recruitment of 53BP1 at TRF2-depleted telomeres (Figure 4D), similarly to what was observed for the inhibition of Ring1b.

To further confirm our findings, we tested whether cells lacking Ring1b would exhibit defects in NHEJ-mediated repair of telomeres. Expression of a dominant-negative allele of TRF2 in Ring1b$^{F/F}$; Rosa26 CRE ER MEFs resulted in DNA damage activation at telomeres in both Ring1b-deficient and Ring1b-proficient cells (Figures 4E and S4E–S4G). In contrast, the occurrence of end-to-end chromosome fusions upon expression of the TRF2 dominant-negative allele was severely reduced in Ring1b-deficient cells (Figure 4F).

Our results suggest that the presence of the heterodimer Ring1b-Bmi1 is required for efficient NHEJ at chromosome ends.

## Ring1b Plays a Critical Role for Efficient DNA Repair of Heterochromatin Loci

Next, we asked whether Ring1b-deficient cells show defective DNA repair throughout the genome. Ring1b null cells were treated with gamma irradiation to induce random DNA damage. As controls, we used wild-type cells and NHEJ-defective cells (Lig4 null) (Kühne et al., 2004). DNA repair efficiency was assayed by fraction of activity released (FAR) assay (Gulston et al., 2002) (Figures S5A and S5B). Our results show that Ring1b null cells do not show any significant defect in DNA repair when compared to wild-type cells. In contrast, Lig4 null cells displayed the expected defect in DNA repair (Figures S5A and S5B). Next, we asked whether Ring1b activity is required for the repair of DNA damage occurring at other heterochromatin loci. To test this hypothesis, we irradiated Ring1b$^{F/F}$; Rosa26 CRE ER MEFs and assayed cells for the persistence of the DNA damage marker γH2AX over time at "chromocenters," cytological distinct structures that correspond to pericentric and centromeric heterochromatin (Guenatri et al., 2004). As a control, we included ATM$^{-/-}$ cells that were previously shown to have a defect in DNA repair at heterochromatin loci (Goodarzi et al., 2008). Our results show that Ring1b null cells, similarly to ATM$^{-/-}$ cells, show a significant persistence of heterochromatin-associated γH2AX foci at 6 hr after irradiation (Figures 5A and 5B). These data suggest that Ring1b activity is required for efficient repair of DNA damage occurring at heterochromatin loci. Notably, at 24 hr postirradiation, Ring1b$^{-/-}$ cells repaired most DNA damage lesions as assessed by γH2AX foci dissipation. In agreement with the FAR assay data, Ring1b$^{-/-}$ cells did not show a defect in DNA repair at nonheterochromatin loci, as shown by the dissipation of γH2AX foci throughout the nuclei (Figure S5C). In conclusion, our data suggest that the role of Ring1b in DNA repair is specific for heterochromatin loci.

## Chromatin Compaction Activity Plays an Important Role for Efficient DNA Repair of Dysfunctional Telomeres

Ring1b is associated to chromatin compaction and gene silencing (Vidal, 2009) and has been shown to be required for the maintenance of a compact chromatin state at *Hox* loci in embryonic stem cells (Eskeland et al., 2010). The chromatin context in which DNA damage occurs has a major impact on the pathway and the efficiency of DNA repair activities, with closed chromatin

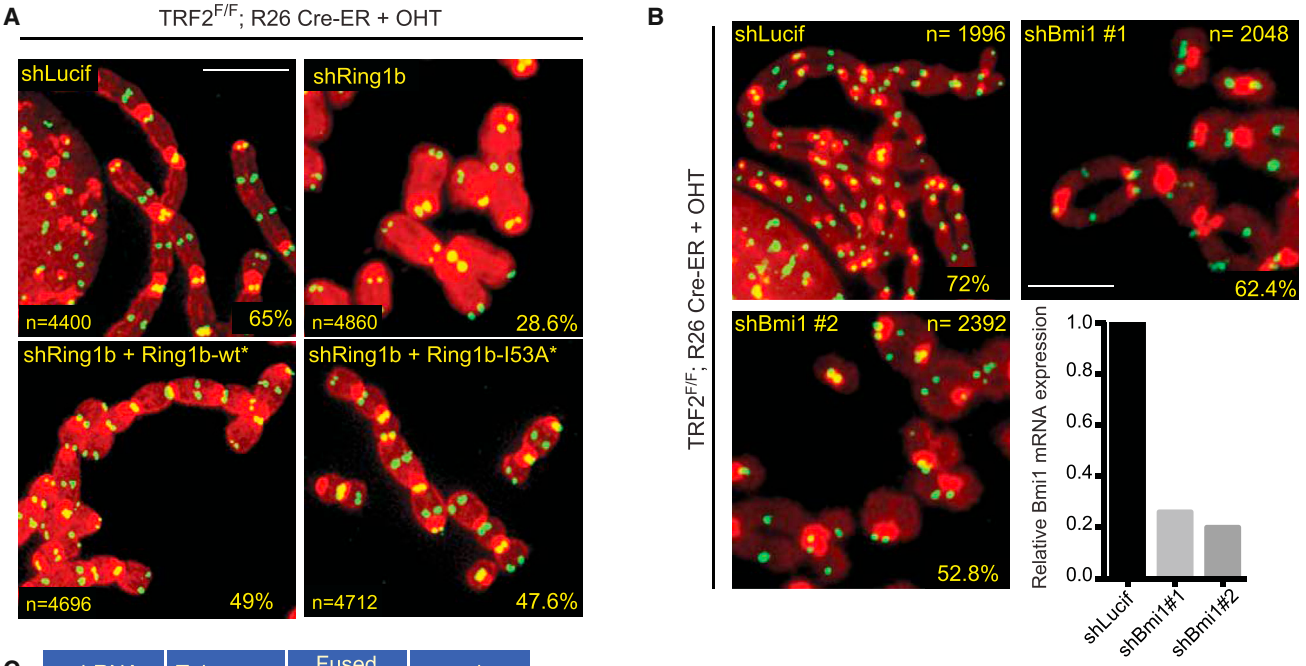


C

| shRNA | Telomeres | Fused Telomeres | p value |
|---|---|---|---|
| shLucif | 1996 | 1434 | control |
| shBmi #1 | 2048 | 1278 | < 0.0001 |
| shBmi1 #2 | 2392 | 1264 | < 0.0001 |

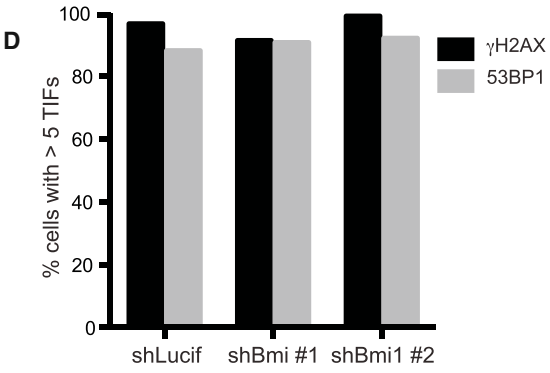


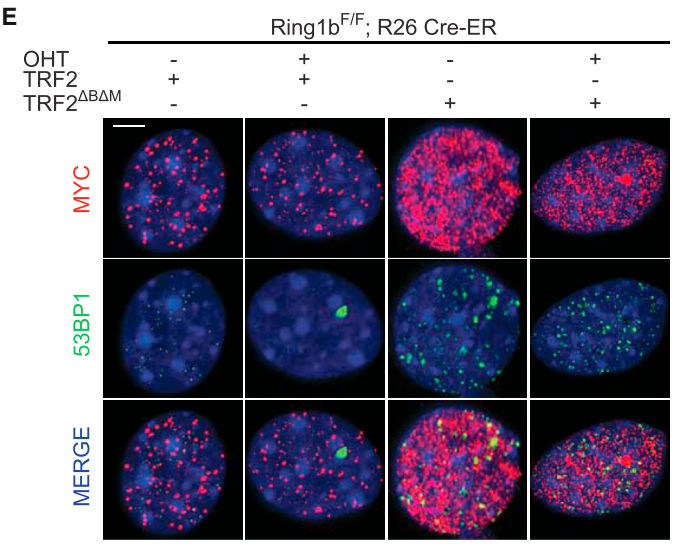


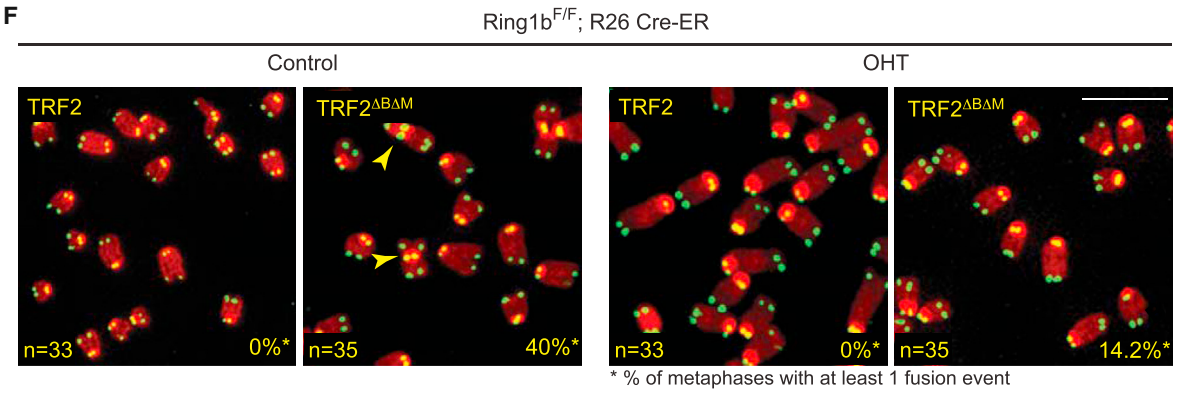


* % of metaphases with at least 1 fusion event

(legend on next page)

favoring the NHEJ pathway (Chiolo et al., 2011; Miller et al., 2010; Soria et al., 2012). We therefore hypothesized that reduced levels of Ring1b could lead to reduced levels of DNA repair at telomeres due to changes in the heterochromatic state. To test this hypothesis, we treated TRF2$^{F/F}$ Rosa CRE-ER MEFs with the histone deacetylase (HDAC) inhibitor trichostatin A (TSA) to decompact chromatin. TSA treatment did not have a significant effect on the recruitment of 53BP1 to TRF2-depleted telomeres (Figure S5D). However, TSA treatment significantly reduced the percentage of telomere fusions (Figure 5C). FACS analysis excluded that TSA treatment affects NHEJ indirectly by altering cell-cycle progression (Figure S5E).

To further validate our hypothesis that loss of chromatin compaction would result in reduction of NHEJ at dysfunctional telomeres, we used Suv39 double-null (dn) MEFs (Peters et al., 2001). The lysine methyltransferases (KMTs) Suv39h1 and Suv39h2 govern H3K9 trimethylation at pericentric heterochromatin (Peters et al., 2001) and were shown to be important for H3K9me3 deposition at telomeres (García-Cao et al., 2004). The presence of trimethylated histone H3 (H3K9me3) is a hallmark of mammalian heterochromatin (Bannister et al., 2001; Lachner et al., 2001; Rea et al., 2000). Suv39 dn cells display loss of heterochromatic features such as loss of heterochromatic association of HP1 proteins and partial decondensation of heterochromatic foci (Lachner et al., 2001; Pinheiro et al., 2012). Expression of a dominant-negative allele of TRF2 in Suv39 dn MEFs also resulted in a lower occurrence of end-to-end chromosome fusions relative to the wild-type control (Figures S5F and S5G). Moreover, shRNA-mediated depletion of the KMT Prdm3, which was shown to prevent Suv39h-mediated H3K9 trimethylation resulting in chromatin decompaction at mouse chromocenters (Pinheiro et al., 2012), significantly reduced the percentage of fused chromosomes in TRF2-deficient cells relative to control cells (Figures 5D and S5H).

Collectively, these results suggest that chromatin compaction is a critical determinant for the frequent occurrence of NHEJ-mediated fusions at dysfunctional telomeres (see schematic model in Figure 5E).

## DISCUSSION

Our data reveal the dynamic changes that occur at the level of chromatin upon the induction of DNA damage at mammalian telomeres. We identified 345 factors that are significantly lost upon TRF2 depletion at telomeric chromatin. These included TRF2 and its associated proteins RAP1 and Apollo. In addition, we identified one factor, CDCA8, that is significantly affected by the removal of TRF2. We identified 471 factors that are present at telomeres regardless of the TRF2 status. These factors included DNA metabolism genes such as histones, DNA polymerases, and telomere-associated proteins that can be recruited to telomeric repeats independently of TRF2 such as the shelterin components TRF1, TIN2, TPP1, and POT1 and the telomere-associated factors ATRX and DAXX (Lewis et al., 2010; Wong et al., 2010). Finally, our isolation identified several known DNA damage response factors that relocalize to telomeres following TRF2 deletion and several additional proteins that were not previously associated with the response to telomere dysfunction. Our validation identified eight proteins that relocalize to dysfunctional telomeres. However, it is important to note that a number of known DNA damage proteins that have been shown to play a crucial role in the response to telomere dysfunction were not identified in our analysis. Notably, RNF8 and RNF168, which are required for the recruitment of 53BP1, are missing from our isolations. This could be explained by the transient nature of the interaction between these ubiquitin ligases at their DNA damage target sites. Nevertheless, the absence of such critical factors represents a limitation of our approach that most likely indicates the lack of other critical factors recruited to dysfunctional telomeres. An additional limitation of the PICh technique for this type of analysis is the requirement for a very large amount of starting material for each individual experiment (over 5 × 10$^8$ cells), which limits the number of conditions and time points that can be tested. In addition, we found a large number of contaminants in our isolations that overlap with the commonly found contaminants in mass spectrometry experiments (Mellacheruvu et al., 2013).

Despite these limitations, this approach represents an unbiased identification of the dynamic changes of chromatin composition upon the onset of DNA damage. As such, the lists of proteins that we identified will represent a valuable resource not only to the telomere biology field but also to researchers studying general DNA repair reactions and genome stability pathways that act throughout the genome.

Finally, we have found a significant role for the polycomb protein Ring1b in the onset of NHEJ at telomeres. These observations further substantiate previous observations of a role for these factors in the response to DNA damage (Chagraoui

**Figure 4. The Ring1b/Bmi1 Heterodimer Acts on the Chromatin at Dysfunctional Telomeres**

(A) Metaphase spreads of TRF2$^{F/F}$ Rosa26 CRE-ER MEFs infected with shLuciferase or shRing1b and Ring1b-WT* or Ring1b-I53A* and treated with OHT for 96 hr. Percentages of fused chromosome ends are indicated. Scale bar represents 5 μm.

(B) Metaphase spreads of TRF2$^{F/F}$ Rosa26 CRE-ER MEFs infected with shRNA constructs directed against Bmi1 and treated with OHT for 96 hr. Percentages of fused chromosome ends are indicated. Scale bar represents 5 μm. Graph shows quantification of relative Bmi1 mRNA levels measured by quantitative PCR, normalized to shLuciferase as control.

(C) Quantification of end-to-end chromosome fusions in (B).

(D) Quantification of γH2AX- and 53BP1-positive TRF2$^{F/F}$ Rosa26 CRE-ER MEFs infected as described in (B), treated with OHT for 72 hr, and fixed and stained for γH2AX and 53BP1 (cells with five or more γH2AX/53BP1 were counted as positive).

(E) Ring1b$^{F/F}$ Rosa26 CRE-ER MEFs (−/+ OHT, 96 hr) were infected with wild-type TRF2 or a TRF2 dominant-negative allele (TRF2$^{\Delta B \Delta M}$) as indicated and fixed and stained for myc (red), 53BP1 (green), and DAPI (blue). Scale bar represents 5 μm.

(F) Metaphase spreads of Ring1b$^{F/F}$ Rosa26 CRE-ER MEFs treated as in (E) were stained for telomeric DNA (green) to detect end-to-end chromosome fusions (arrowheads). Number of metaphases analyzed and percentage of metaphases with at least one fusion event are indicated. Scale bar represents 5 μm.

See also Figure S4.

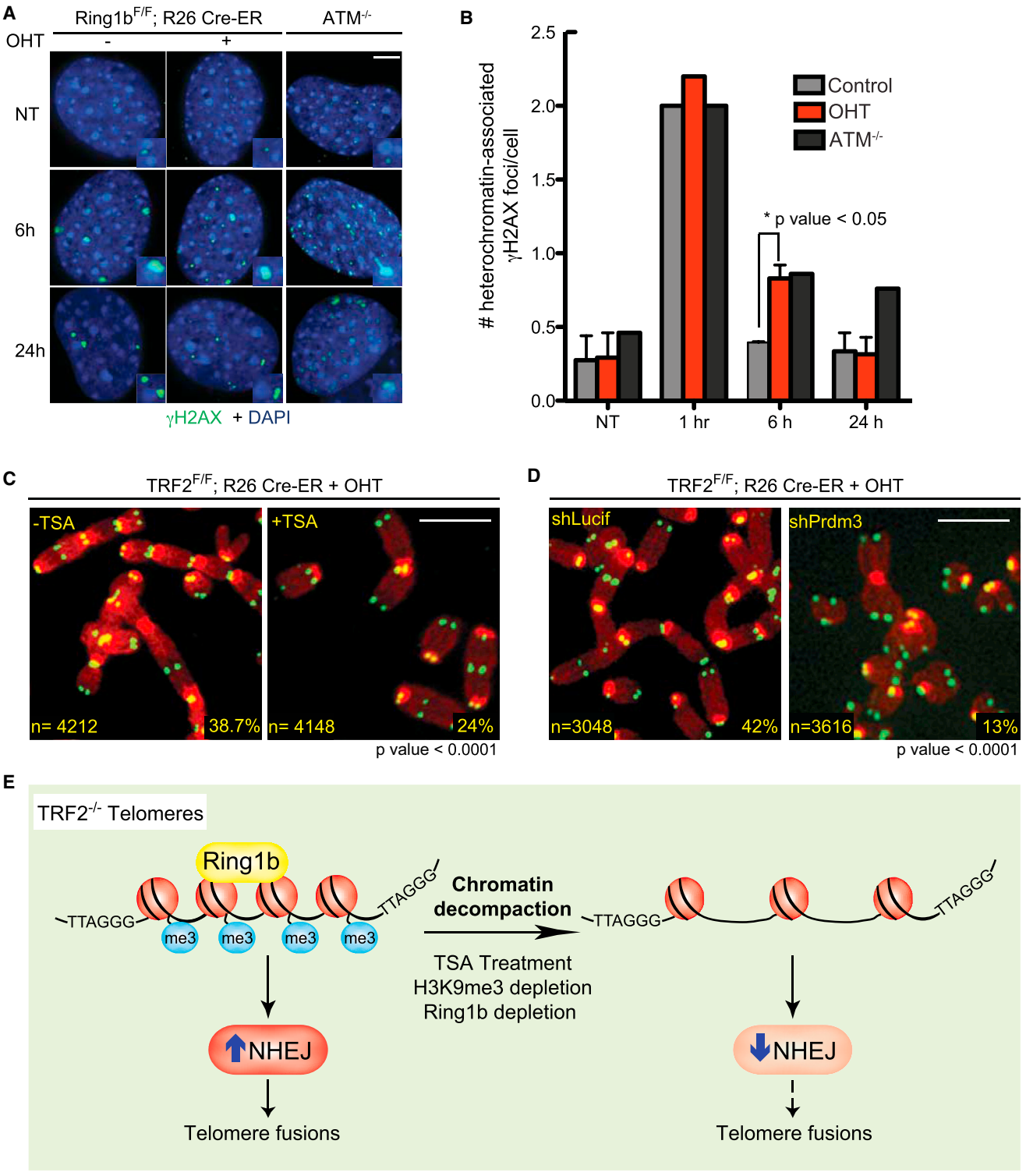


**Figure 5. Compact Chromatin Favors NHEJ-Mediated Repair of Dysfunctional Telomeres**

(A) Confluent, stationary-phase Ring1b$^{F/F}$ Rosa26 CRE-ER MEFs untreated or treated with tamoxifen (−/+ OHT) were left untreated (NT) or irradiated (2 Gy) and harvested at the indicated time points postirradiation. ATM$^{-/-}$ MEFs were used as a control. Cells were fixed and stained for γH2AX (green) and DAPI (blue). Scale bar represents 5 μm.

(B) Quantification of the total number of heterochromatin-associated γH2AX foci in cells treated as described in (A). Error bars represent SD of the average of three independent experiments.

*(legend continued on next page)*

et al., 2011; Chou et al., 2010; Facchino et al., 2010; Ginjala et al., 2011; Ismail et al., 2010). Strikingly, however, our data suggest that in the absence of Ring1b, the signaling events downstream of ATM activation such as γH2AX and 53BP1 recruitment are not affected. These data are in agreement with the observation that recruitment of 53BP1 is independent of Ring1b-mediated H2A ubiquitylation (Gatti et al., 2012; Mattiroli et al., 2012).

Our data suggest that Ring1b plays a critical role to maintain a compact chromatin status that is permissive for NHEJ. Indeed, previous reports have shown that compact chromatin is more prone to undergo NHEJ-mediated DNA repair (Chiolo et al., 2011; Miller et al., 2010). Ring1b activity in chromatin compaction has been well established in the context of gene expression at *Hox* loci (Eskeland et al., 2010). Notably, it has been reported that the E3 activity of Ring1b is not required for chromatin compaction, similarly to what we found in the context of promotion of NHEJ at dysfunctional telomeres. We found that treatment of cells with the HDAC inhibitor TSA resulted in reduced levels of NHEJ at telomeres, thus further suggesting that chromatin compaction is critical for NHEJ at dysfunctional telomeres. Similarly, we found that reducing H3K9me3 levels in cells depleted of TRF2, either by depletion of Prdm3 or by the use of Suv39 dn MEFs, impaired the formation of NHEJ-mediated end-to-end chromosome fusions. These results are in agreement with previous results showing a role for HDAC1 and HDAC2 in NHEJ-dependent DNA repair at genome-wide sites of DNA lesion (Miller et al., 2010) as well as with the observation that TSA treatment shifts the repair choice toward the homologous recombination pathway (Tang et al., 2013). The heterochromatic status of telomeres would therefore explain why telomere dysfunction preferentially triggers NHEJ-mediated DNA repair and suggests that alterations in chromatin status could be responsible for the increased homologous recombination observed at telomeres in tumors that engage the alternative telomere-lengthening (ALT) pathway (Cesare and Reddel, 2008). In line with this hypothesis, increased rates of telomere sister chromatid exchange were recently reported in ALT tumor cells subjected to TSA treatment (Jung et al., 2013).

## EXPERIMENTAL PROCEDURES

### Telomeric Chromatin Isolation by PICh

Proteomics of isolated chromatin segments (PICh) was carried out as previously described (Déjardin and Kingston, 2009) with the following modifications: $5 \times 10^8$ MEFs were used per sample, and two sonication cycles were performed using a Misonix S-4000 (first cycle, power 70%; second cycle, power 40%). Each cycle consisted of 15 s on and 45 s off for a total process time of 2 min. For hybridization with telomeric probe, a PNA probe (0.6 μM) was used (desthiobiotin-112 atoms spacer-TTAGGGTTAGGGTTAGGGTTAGGG) using the conditions described before, with the exception that denaturation was carried out at 65°C for 6 min.

### Mass Spectrometry Analysis

For mass spectrometry, analysis samples were denatured, reduced, and alkylated prior to an overnight digestion with trypsin. Peptide mixtures were analyzed by nanoflow liquid chromatography mass spectrometry using an Eksigent nanopump and LTQ-Orbitrap mass spectrometer (Thermo Scientific) using a seven-step MudPIT separation. Tandem MS spectra were collected in a data-dependent fashion, and resulting spectra were extracted using RawXtract. Protein identification was done with Integrated Proteomics Pipeline (IP2) by searching against UniProt Human database and filtering to 1% false positive at the spectrum level using DTASelect.

### MEFs and shRNA Infections

$TRF2^{F/F}$ Rosa26 CRE-ER MEFs were previously described (Okamoto et al., 2013). $Ring1b^{F/F}$ Rosa CRE ER MEFs were derived from a cross between Ring1b conditional mice (de Napoles et al., 2004) and Rosa26 CRE-ER mice (Ventura et al., 2007). CRE activation was obtained treating cells with 4-hydroxytamoxifen (OHT) at a final concentration of 0.6 μM. Suv39 dn immortalized MEFs (iMEFs) and wild-type control iMEFs were a kind gift from T. Jenuwein.

shRNAs were cloned into the pLKO-puromycin lentiviral vector (for sequences see Supplemental Experimental Procedures). shRNA infections were performed as previously described (Okamoto et al., 2013). Knockdown efficiency was analyzed by quantitative PCR using Roche Sybr Green Mastermix according to the manufacturer's instructions on a LightCycler 480 II (Roche).

### Immunofluorescence, IF-FISH, ChIP, and Immunoblotting

Immunoblots and IF were performed using the protocols described previously (Celli and de Lange, 2005). For Ring1b detection by immunoblot, extracts were prepared according to Vella et al. (2013). For IF, where indicated cells were permeabilized with Triton X-100 buffer (for details, see the Supplemental Experimental Procedures). Fluorescence in situ hybridization immunofluorescence (FISH-IF) staining was performed using the protocol developed by Sedivy and colleagues (Herbig et al., 2004). For quantification, at least 100 cells were counted following FISH-IF analysis. Cells with at least five foci colocalizing with telomere DNA or TRF1 were scored as positive. Error bars indicate SDs and derive from averages of three independent experiments. p values were calculated using the Student's t test.

ChIP experiments were performed as described previously (Loayza and De Lange, 2003; O'Sullivan et al., 2010; Ye and de Lange, 2004). Full details of all other experimental procedures are given in the Supplemental Experimental Procedures.

## SUPPLEMENTAL INFORMATION

Supplemental Information includes Supplemental Experimental Procedures, five figures, and three tables and can be found with this article online at http://dx.doi.org/10.1016/j.celrep.2014.04.002.

## ACKNOWLEDGMENTS

We thank Michael Nicholas Boddy, Sara Buonomo, Titia de Lange, Ronald Hay, Thomas Jenuwein, Akio Koizumi, Yoko Koseki, Agnel Sfeir, and Bertrand Tan for providing critical reagents. We thank Jerome Dejardin for suggestions on PICh purification. We are grateful to Claire Attwooll, Daniele Fachinetti, Kyle Miller, and Agnel Sfeir for critical reading of the manuscript. This work was supported by a Pew Scholars Award (E.L.D.), the Novartis Advanced Discovery Institute (E.L.D.), NIH AG038677 (E.L.D.), P41 GM103533 (J.R.Y.), the Italian

(C) Metaphase spreads of $TRF2^{F/F}$ Rosa26 CRE-ER MEFs treated with OHT for 72 hr and, when indicated, with TSA (18 hr). Percentages of fused chromosome ends are indicated. Scale bar represents 5 μm.
(D) Metaphase spreads of $TRF2^{F/F}$ Rosa26 CRE-ER MEFs infected with an shRNA against Prdm3 (shPrdm3) or a control shRNA (shLuciferase) and treated with OHT for 72 hr. Scale bar represents 5 μm.
(E) Model for the role of chromatin compaction in NHEJ-mediated repair of dysfunctional telomeres.
See also Figure S5.

Association for Cancer Research and the Italian Ministry of Health (D.P.), and a fellowship from FIRC (A.P.).

Received: October 18, 2013
Revised: March 4, 2014
Accepted: April 2, 2014
Published: May 8, 2014

## REFERENCES

Artandi, S.E., Chang, S., Lee, S.L., Alson, S., Gottlieb, G.J., Chin, L., and DePinho, R.A. (2000). Telomere dysfunction promotes non-reciprocal translocations and epithelial cancers in mice. Nature *406*, 641–645.

Attwooll, C.L., Akpinar, M., and Petrini, J.H. (2009). The mre11 complex and the response to dysfunctional telomeres. Mol. Cell. Biol. *29*, 5540–5551.

Augereau, A., T'kint de Roodenbeke, C., Simonet, T., Bauwens, S., Horard, B., Callanan, M., Leroux, D., Jallades, L., Salles, G., Gilson, E., and Poncet, D. (2011). Telomeric damage in early stage of chronic lymphocytic leukemia correlates with shelterin dysregulation. Blood *118*, 1316–1322.

Bannister, A.J., Zegerman, P., Partridge, J.F., Miska, E.A., Thomas, J.O., Allshire, R.C., and Kouzarides, T. (2001). Selective recognition of methylated lysine 9 on histone H3 by the HP1 chromo domain. Nature *410*, 120–124.

Buchwald, G., van der Stoop, P., Weichenrieder, O., Perrakis, A., van Lohuizen, M., and Sixma, T.K. (2006). Structure and E3-ligase activity of the Ring-Ring complex of polycomb proteins Bmi1 and Ring1b. EMBO J. *25*, 2465–2474.

Buscemi, G., Perego, P., Carenini, N., Nakanishi, M., Chessa, L., Chen, J., Khanna, K., and Delia, D. (2004). Activation of ATM and Chk2 kinases in relation to the amount of DNA strand breaks. Oncogene *23*, 7691–7700.

Cao, R., Tsukada, Y., and Zhang, Y. (2005). Role of Bmi-1 and Ring1A in H2A ubiquitylation and Hox gene silencing. Mol. Cell *20*, 845–854.

Carmena, M., Wheelock, M., Funabiki, H., and Earnshaw, W.C. (2012). The chromosomal passenger complex (CPC): from easy rider to the godfather of mitosis. Nat. Rev. Mol. Cell Biol. *13*, 789–803.

Celli, G.B., and de Lange, T. (2005). DNA processing is not required for ATM-mediated telomere damage response after TRF2 deletion. Nat. Cell Biol. *7*, 712–718.

Cesare, A.J., and Reddel, R.R. (2008). Telomere uncapping and alternative lengthening of telomeres. Mech. Ageing Dev. *129*, 99–108.

Chagraoui, J., Hébert, J., Girard, S., and Sauvageau, G. (2011). An anticlastogenic function for the Polycomb Group gene Bmi1. Proc. Natl. Acad. Sci. USA *108*, 5284–5289.

Chan, K.M., and Zhang, Z. (2012). Leucine-rich repeat and WD repeat-containing protein 1 is recruited to pericentric heterochromatin by trimethylated lysine 9 of histone H3 and maintains heterochromatin silencing. J. Biol. Chem. *287*, 15024–15033.

Chapman, J.R., Barral, P., Vannier, J.B., Borel, V., Steger, M., Tomas-Loba, A., Sartori, A.A., Adams, I.R., Batista, F.D., and Boulton, S.J. (2013). RIF1 is essential for 53BP1-dependent nonhomologous end joining and suppression of DNA double-strand break resection. Mol. Cell *49*, 858–871.

Chin, L., Artandi, S.E., Shen, Q., Tam, A., Lee, S.L., Gottlieb, G.J., Greider, C.W., and DePinho, R.A. (1999). p53 deficiency rescues the adverse effects of telomere loss and cooperates with telomere dysfunction to accelerate carcinogenesis. Cell *97*, 527–538.

Chin, K., de Solorzano, C.O., Knowles, D., Jones, A., Chou, W., Rodriguez, E.G., Kuo, W.L., Ljung, B.M., Chew, K., Myambo, K., et al. (2004). In situ analyses of genome instability in breast cancer. Nat. Genet. *36*, 984–988.

Chiolo, I., Minoda, A., Colmenares, S.U., Polyzos, A., Costes, S.V., and Karpen, G.H. (2011). Double-strand breaks in heterochromatin move outside of a dynamic HP1a domain to complete recombinational repair. Cell *144*, 732–744.

Chou, D.M., Adamson, B., Dephoure, N.E., Tan, X., Nottke, A.C., Hurov, K.E., Gygi, S.P., Colaiácovo, M.P., and Elledge, S.J. (2010). A chromatin localization screen reveals poly (ADP ribose)-regulated recruitment of the repressive polycomb and NuRD complexes to sites of DNA damage. Proc. Natl. Acad. Sci. USA *107*, 18475–18480.

d'Adda di Fagagna, F., Reaper, P.M., Clay-Farrace, L., Fiegler, H., Carr, P., Von Zglinicki, T., Saretzki, G., Carter, N.P., and Jackson, S.P. (2003). A DNA damage checkpoint response in telomere-initiated senescence. Nature *426*, 194–198.

de Lange, T. (2005). Shelterin: the protein complex that shapes and safeguards human telomeres. Genes Dev. *19*, 2100–2110.

de Napoles, M., Mermoud, J.E., Wakao, R., Tang, Y.A., Endoh, M., Appanah, R., Nesterova, T.B., Silva, J., Otte, A.P., Vidal, M., et al. (2004). Polycomb group proteins Ring1A/B link ubiquitylation of histone H2A to heritable gene silencing and X inactivation. Dev. Cell *7*, 663–676.

Déjardin, J., and Kingston, R.E. (2009). Purification of proteins associated with specific genomic Loci. Cell *136*, 175–186.

Denchi, E.L., and de Lange, T. (2007). Protection of telomeres through independent control of ATM and ATR by TRF2 and POT1. Nature *448*, 1068–1071.

Di Virgilio, M., Callen, E., Yamane, A., Zhang, W., Jankovic, M., Gitlin, A.D., Feldhahn, N., Resch, W., Oliveira, T.Y., Chait, B.T., et al. (2013). Rif1 prevents resection of DNA breaks and promotes immunoglobulin class switching. Science *339*, 711–715.

Dimitrova, N., and de Lange, T. (2006). MDC1 accelerates nonhomologous end-joining of dysfunctional telomeres. Genes Dev. *20*, 3238–3243.

Dimitrova, N., and de Lange, T. (2009). Cell cycle-dependent role of MRN at dysfunctional telomeres: ATM signaling-dependent induction of nonhomologous end joining (NHEJ) in G1 and resection-mediated inhibition of NHEJ in G2. Mol. Cell. Biol. *29*, 5552–5563.

Dimitrova, N., Chen, Y.C., Spector, D.L., and de Lange, T. (2008). 53BP1 promotes non-homologous end joining of telomeres by increasing chromatin mobility. Nature *456*, 524–528.

Dokal, I. (2000). Dyskeratosis congenita in all its forms. Br. J. Haematol. *110*, 768–779.

Escribano-Díaz, C., Orthwein, A., Fradet-Turcotte, A., Xing, M., Young, J.T., Tkáč, J., Cook, M.A., Rosebrock, A.P., Munro, M., Canny, M.D., et al. (2013). A cell cycle-dependent regulatory circuit composed of 53BP1-RIF1 and BRCA1-CtIP controls DNA repair pathway choice. Mol. Cell *49*, 872–883.

Eskeland, R., Leeb, M., Grimes, G.R., Kress, C., Boyle, S., Sproul, D., Gilbert, N., Fan, Y., Skoultchi, A.I., Wutz, A., and Bickmore, W.A. (2010). Ring1B compacts chromatin structure and represses gene expression independent of histone ubiquitination. Mol. Cell *38*, 452–464.

Facchino, S., Abdouh, M., Chatoo, W., and Bernier, G. (2010). BMI1 confers radioresistance to normal and cancerous neural stem cells through recruitment of the DNA damage response machinery. J. Neurosci. *30*, 10096–10111.

García-Cao, M., O'Sullivan, R., Peters, A.H., Jenuwein, T., and Blasco, M.A. (2004). Epigenetic regulation of telomere length in mammalian cells by the Suv39h1 and Suv39h2 histone methyltransferases. Nat. Genet. *36*, 94–99.

Gatti, M., Pinato, S., Maspero, E., Soffientini, P., Polo, S., and Penengo, L. (2012). A novel ubiquitin mark at the N-terminal tail of histone H2As targeted by RNF168 ubiquitin ligase. Cell Cycle *11*, 2538–2544.

Ginjala, V., Nacerddine, K., Kulkarni, A., Oza, J., Hill, S.J., Yao, M., Citterio, E., van Lohuizen, M., and Ganesan, S. (2011). BMI1 is recruited to DNA breaks and contributes to DNA damage-induced H2A ubiquitination and repair. Mol. Cell. Biol. *31*, 1972–1982.

Goodarzi, A.A., Noon, A.T., Deckbar represents, D., Ziv, Y., Shiloh, Y., Löbrich, M., and Jeggo, P.A. (2008). ATM signaling facilitates repair of DNA double-strand breaks associated with heterochromatin. Mol. Cell *31*, 167–177.

Gordon, K.E., Ireland, H., Roberts, M., Steeghs, K., McCaul, J.A., MacDonald, D.G., and Parkinson, E.K. (2003). High levels of telomere dysfunction bestow a selective disadvantage during the progression of human oral squamous cell carcinoma. Cancer Res. *63*, 458–467.

Grolimund, L., Aeby, E., Hamelin, R., Armand, F., Chiappe, D., Moniatte, M., and Lingner, J. (2013). A quantitative telomeric chromatin isolation protocol identifies different telomeric states. Nat Commun *4*, 2848.

Guenatri, M., Bailly, D., Maison, C., and Almouzni, G. (2004). Mouse centric and pericentric satellite repeats form distinct functional heterochromatin. J. Cell Biol. *166*, 493–505.

Gulston, M., Fulford, J., Jenner, T., de Lara, C., and O'Neill, P. (2002). Clustered DNA damage induced by gamma radiation in human fibroblasts (HF19), hamster (V79-4) cells and plasmid DNA is revealed as Fpg and Nth sensitive sites. Nucleic Acids Res. *30*, 3464–3472.

Hastie, N.D., Dempster, M., Dunlop, M.G., Thompson, A.M., Green, D.K., and Allshire, R.C. (1990). Telomere reduction in human colorectal carcinoma and with ageing. Nature *346*, 866–868.

Herbig, U., Jobling, W.A., Chen, B.P., Chen, D.J., and Sedivy, J.M. (2004). Telomere shortening triggers senescence of human cells through a pathway involving ATM, p53, and p21(CIP1), but not p16(INK4a). Mol. Cell *14*, 501–513.

Ismail, I.H., Andrin, C., McDonald, D., and Hendzel, M.J. (2010). BMI1-mediated histone ubiquitylation promotes DNA double-strand break repair. J. Cell Biol. *191*, 45–60.

Jung, A.R., Yoo, J.E., Shim, Y.H., Choi, Y.N., Jeung, H.C., Chung, H.C., Rha, S.Y., and Oh, B.K. (2013). Increased alternative lengthening of telomere phenotypes of telomerase-negative immortal cells upon trichostatin—a treatment. Anticancer Res. *33*, 821–829.

Kirwan, M., and Dokal, I. (2009). Dyskeratosis congenita, stem cells and telomeres. Biochim. Biophys. Acta *1792*, 371–379.

Kühne, M., Riballo, E., Rief, N., Rothkamm, K., Jeggo, P.A., and Löbrich, M. (2004). A double-strand break repair defect in ATM-deficient cells contributes to radiosensitivity. Cancer Res. *64*, 500–508.

Lachner, M., O'Carroll, D., Rea, S., Mechtler, K., and Jenuwein, T. (2001). Methylation of histone H3 lysine 9 creates a binding site for HP1 proteins. Nature *410*, 116–120.

Lenain, C., Bauwens, S., Amiard, S., Brunori, M., Giraud-Panis, M.J., and Gilson, E. (2006). The Apollo 5′ exonuclease functions together with TRF2 to protect telomeres from DNA repair. Curr. Biol. *16*, 1303–1310.

Lewis, P.W., Elsaesser, S.J., Noh, K.M., Stadler, S.C., and Allis, C.D. (2010). Daxx is an H3.3-specific histone chaperone and cooperates with ATRX in replication-independent chromatin assembly at telomeres. Proc. Natl. Acad. Sci. USA *107*, 14075–14080.

Li, B., Oestreich, S., and de Lange, T. (2000). Identification of human Rap1: implications for telomere evolution. Cell *101*, 471–483.

Lin, T.T., Letsolo, B.T., Jones, R.E., Rowson, J., Pratt, G., Hewamana, S., Fegan, C., Pepper, C., and Baird, D.M. (2010). Telomere dysfunction and fusion during the progression of chronic lymphocytic leukemia: evidence for a telomere crisis. Blood *116*, 1899–1907.

Loayza, D., and De Lange, T. (2003). POT1 as a terminal transducer of TRF1 telomere length control. Nature *423*, 1013–1018.

Maser, R.S., and DePinho, R.A. (2002). Keeping telomerase in its place. Nat. Med. *8*, 934–936.

Mattiroli, F., Vissers, J.H., van Dijk, W.J., Ikpa, P., Citterio, E., Vermeulen, W., Marteijn, J.A., and Sixma, T.K. (2012). RNF168 ubiquitinates K13-15 on H2A/H2AX to drive DNA damage signaling. Cell *150*, 1182–1195.

Meeker, A.K., Hicks, J.L., Iacobuzio-Donahue, C.A., Montgomery, E.A., Westra, W.H., Chan, T.Y., Ronnett, B.M., and De Marzo, A.M. (2004). Telomere length abnormalities occur early in the initiation of epithelial carcinogenesis. Clin. Cancer Res. *10*, 3317–3326.

Mellacheruvu, D., Wright, Z., Couzens, A.L., Lambert, J.P., St-Denis, N.A., Li, T., Miteva, Y.V., Hauri, S., Sardiu, M.E., Low, T.Y., et al. (2013). The CRAPome: a contaminant repository for affinity purification-mass spectrometry data. Nat. Methods *10*, 730–736.

Miller, K.M., Tjeertes, J.V., Coates, J., Legube, G., Polo, S.E., Britton, S., and Jackson, S.P. (2010). Human HDAC1 and HDAC2 function in the DNA-damage response to promote DNA nonhomologous end-joining. Nat. Struct. Mol. Biol. *17*, 1144–1151.

Mitchell, J.R., Wood, E., and Collins, K. (1999). A telomerase component is defective in the human disease dyskeratosis congenita. Nature *402*, 551–555.

O'Sullivan, R.J., Kubicek, S., Schreiber, S.L., and Karlseder, J. (2010). Reduced histone biosynthesis and chromatin changes arising from a damage signal at telomeres. Nat. Struct. Mol. Biol. *17*, 1218–1225.

Okamoto, K., Bartocci, C., Ouzounov, I., Diedrich, J.K., Yates, J.R., 3rd, and Denchi, E.L. (2013). A two-step mechanism for TRF2-mediated chromosome-end protection. Nature *494*, 502–505.

Peters, A.H., O'Carroll, D., Scherthan, H., Mechtler, K., Sauer, S., Schöfer, C., Weipoltshammer, K., Pagani, M., Lachner, M., Kohlmaier, A., et al. (2001). Loss of the Suv39h histone methyltransferases impairs mammalian heterochromatin and genome stability. Cell *107*, 323–337.

Peuscher, M.H., and Jacobs, J.J. (2011). DNA-damage response and repair activities at uncapped telomeres depend on RNF8. Nat. Cell Biol. *13*, 1139–1145.

Pfeiffer, V., Crittin, J., Grolimund, L., and Lingner, J. (2013). The THO complex component Thp2 counteracts telomeric R-loops and telomere shortening. EMBO J. *32*, 2861–2871.

Pinheiro, I., Margueron, R., Shukeir, N., Eisold, M., Fritzsch, C., Richter, F.M., Mittler, G., Genoud, C., Goyama, S., Kurokawa, M., et al. (2012). Prdm3 and Prdm16 are H3K9me1 methyltransferases required for mammalian heterochromatin integrity. Cell *150*, 948–960.

Ramsay, A.J., Quesada, V., Foronda, M., Conde, L., Martínez-Trillos, A., Villamor, N., Rodríguez, D., Kwarciak, A., Garabaya, C., Gallardo, M., et al. (2013). POT1 mutations cause telomere dysfunction in chronic lymphocytic leukemia. Nat. Genet. *45*, 526–530.

Rea, S., Eisenhaber, F., O'Carroll, D., Strahl, B.D., Sun, Z.W., Schmid, M., Opravil, S., Mechtler, K., Ponting, C.P., Allis, C.D., and Jenuwein, T. (2000). Regulation of chromatin structure by site-specific histone H3 methyltransferases. Nature *406*, 593–599.

Rudolph, K.L., Millard, M., Bosenberg, M.W., and DePinho, R.A. (2001). Telomere dysfunction and evolution of intestinal carcinoma in mice and humans. Nat. Genet. *28*, 155–159.

Sarper, N., Zengin, E., and Kılıç, S.C. (2010). A child with severe form of dyskeratosis congenita and TINF2 mutation of shelterin complex. Pediatr. Blood Cancer *55*, 1185–1186.

Shay, J.W., and Wright, W.E. (1999). Mutant dyskerin ends relationship with telomerase. Science *286*, 2284–2285.

Shay, J.W., and Wright, W.E. (2001). Telomeres and telomerase: implications for cancer and aging. Radiat. Res. *155*, 188–193.

Shen, Z., Sathyan, K.M., Geng, Y., Zheng, R., Chakraborty, A., Freeman, B., Wang, F., Prasanth, K.V., and Prasanth, S.G. (2010). A WD-repeat protein stabilizes ORC binding to chromatin. Mol. Cell *40*, 99–111.

Soria, G., Polo, S.E., and Almouzni, G. (2012). Prime, repair, restore: the active role of chromatin in the DNA damage response. Mol. Cell *46*, 722–734.

Stock, J.K., Giadrossi, S., Casanova, M., Brookes, E., Vidal, M., Koseki, H., Brockdorff, N., Fisher, A.G., and Pombo, A. (2007). Ring1-mediated ubiquitination of H2A restrains poised RNA polymerase II at bivalent genes in mouse ES cells. Nat. Cell Biol. *9*, 1428–1435.

Suram, A., Kaplunov, J., Patel, P.L., Ruan, H., Cerutti, A., Boccardi, V., Fumagalli, M., Di Micco, R., Mirani, N., Gurung, R.L., et al. (2012). Oncogene-induced telomere dysfunction enforces cellular senescence in human cancer precursor lesions. EMBO J. *31*, 2839–2851.

Takai, H., Smogorzewska, A., and de Lange, T. (2003). DNA damage foci at dysfunctional telomeres. Curr. Biol. *13*, 1549–1556.

Tang, J., Cho, N.W., Cui, G., Manion, E.M., Shanbhag, N.M., Botuyan, M.V., Mer, G., and Greenberg, R.A. (2013). Acetylation limits 53BP1 association with damaged chromatin to promote homologous recombination. Nat. Struct. Mol. Biol. *20*, 317–325.

Touzot, F., Callebaut, I., Soulier, J., Gaillard, L., Azerrad, C., Durandy, A., Fischer, A., de Villartay, J.P., and Revy, P. (2010). Function of Apollo (SNM1B) at telomere highlighted by a splice variant identified in a patient with Hoyeraal-Hreidarsson syndrome. Proc. Natl. Acad. Sci. USA *107*, 10097–10102.

van Overbeek, M., and de Lange, T. (2006). Apollo, an Artemis-related nuclease, interacts with TRF2 and protects human telomeres in S phase. Curr. Biol. *16*, 1295–1302.

Vella, P., Scelfo, A., Jammula, S., Chiacchiera, F., Williams, K., Cuomo, A., Roberto, A., Christensen, J., Bonaldi, T., Helin, K., and Pasini, D. (2013). Tet proteins connect the O-linked N-acetylglucosamine transferase Ogt to chromatin in embryonic stem cells. Mol. Cell *49*, 645–656.

Ventura, A., Kirsch, D.G., McLaughlin, M.E., Tuveson, D.A., Grimm, J., Lintault, L., Newman, J., Reczek, E.E., Weissleder, R., and Jacks, T. (2007). Restoration of p53 function leads to tumour regression in vivo. Nature *445*, 661–665.

Vidal, M. (2009). Role of polycomb proteins Ring1A and Ring1B in the epigenetic regulation of gene expression. Int. J. Dev. Biol. *53*, 355–370.

Vulliamy, T., Marrone, A., Szydlo, R., Walne, A., Mason, P.J., and Dokal, I. (2004). Disease anticipation is associated with progressive telomere shortening in families with dyskeratosis congenita due to mutations in TERC. Nat. Genet. *36*, 447–449.

Walne, A.J., Vulliamy, T., Beswick, R., Kirwan, M., and Dokal, I. (2008). TINF2 mutations result in very short telomeres: analysis of a large cohort of patients with dyskeratosis congenita and related bone marrow failure syndromes. Blood *112*, 3594–3600.

Wang, H., Wang, L., Erdjument-Bromage, H., Vidal, M., Tempst, P., Jones, R.S., and Zhang, Y. (2004). Role of histone H2A ubiquitination in Polycomb silencing. Nature *431*, 873–878.

Wang, M., Weiss, M., Simonovic, M., Haertinger, G., Schrimpf, S.P., Hengartner, M.O., and von Mering, C. (2012). PaxDb, a database of protein abundance averages across all three domains of life. Mol. Cell. Proteomics *11*, 492–500.

Wong, L.H., McGhie, J.D., Sim, M., Anderson, M.A., Ahn, S., Hannan, R.D., George, A.J., Morgan, K.A., Mann, J.R., and Choo, K.H. (2010). ATRX interacts with H3.3 in maintaining telomere structural integrity in pluripotent embryonic stem cells. Genome Res. *20*, 351–360.

Ye, J.Z., and de Lange, T. (2004). TIN2 is a tankyrase 1 PARP modulator in the TRF1 telomere length control complex. Nat. Genet. *36*, 618–623.

Zimmermann, M., Lottersberger, F., Buonomo, S.B., Sfeir, A., and de Lange, T. (2013). 53BP1 regulates DSB repair using Rif1 to control 5′ end resection. Science *339*, 700–704.